Beam Optics of Quadrupole Probe-forming Systems

Beam Optics of Quadrupole Probe-Forming Systems

G W Grime
F Watt
Department of Nuclear Physics, University of Oxford

Adam Hilger Ltd, Bristol

British Library Cataloguing in Publication Data

Grime, G. W.
Beam optics of quadrupole probe–forming systems
1. Beam optics
I. Title II. Watt, F.
530.1'41 QC665.B/

ISBN 0-85274-546-X

Consultant Editor: **Professor G Dearnaley**

Published by Adam Hilger Ltd, Techno House, Redcliffe Way, Bristol BS1 6NX.
The Adam Hilger book-publishing imprint is owned by The Institute of Physics.

Printed in Great Britain by J W Arrowsmith Limited, Bristol

Preface

During the last decade, the use of high-energy ion beams for the purpose of elemental analysis has increased enormously, for by using the three techniques of particle-induced x-ray emission (PIXE), Rutherford backscattering (RBS) and nuclear reaction analysis (PRA), the elemental composition of a sample may be determined with sensitivities in the parts per million region.

The use of focused high-energy ion beams or microprobes to provide information on the distribution of elements in a sample is an obvious development of the technique, and since the first microprobe was constructed at Harwell in the early 1970s there has been a slow but steady increase in the number of these instruments throughout the world. There is no doubt that the ion microprobe will prove to be of great importance in a broad range of analytical applications.

That the field of ion microprobes has not expanded faster is primarily due to two factors. The first is that the production of ions with energies suitable for PIXE, RBS and PRA requires at least a million-volt particle accelerator, and thus the majority of microprobes tend to be found only in the nuclear structure or physics laboratories which have such accelerators available. The second factor concerns the relative complexity of focusing such high-energy ions to form a probe. The high rigidity of ions with energies of several MeV means that the successful technology developed for the electron microscope cannot be used and the focusing can only be achieved using stronger focusing elements such as quadrupole lenses.

Although quadrupole lenses have been used for many years as beam transport devices, their application to probe formation is largely unknown. The available literature on quadrupole lenses tends to be theoretical in nature, and although a few configurations with simplifying symmetry have been investigated, the results are not directly applicable to the design of practical ion microprobe systems.

This book is an attempt to present the theory of quadrupole focusing with the practical development of microprobe systems in mind. The introductory chapter outlines the analytical processes mentioned above and provides a background to the problems of designing quadrupole probe-forming systems. Following a description of the quadrupole lens and the mathematical models used to describe the fields within both magnetic and electrostatic quadrupole lenses (chapter 2), we describe two

techniques for calculating the path of a charged particle through a beam-optical system; matrix methods (chapter 3) and numerical raytracing (chapter 4). Both of these techniques are derived from the equation of motion, but rather than attempting to extract general results directly from the theory, the emphasis in these chapters is on demonstrating how the theory may be used to develop computer programs for the design of microprobe systems.

As a guide to the design of the quadrupole microprobe systems, the intrinsic beam-optical parameters of a large number of quadrupole configurations have been calculated and are presented graphically and in tabular form in Appendix 1. Chapter 5 describes how the appendix may be used to estimate the resulting spot size for any of the wide range of doublet, triplet and quadruplet systems investigated.

The minimum spot size achieved by a quadrupole system is influenced strongly by parasitic aberrations due to imperfections in the construction and alignment of the instrument. Due to the large number of parameters involved, it is not possible to investigate parasitic aberrations systematically as was done for the intrinsic properties and so in chapter 6 we have attempted to assess the importance of the various effects by reference to their influence in three existing microprobe systems.

Finally, in chapter 7, we describe briefly some novel and interesting alternatives to the quadrupole lens as the focusing element and also discuss ways in which the focused ion beam may be further reduced in size.

Unfortunately, due to limitations of space we have not been able to consider the hardware associated with high-energy ion microprobes or any of the many applications which have been reported. It is hoped, however, that sufficient references to the literature have been included to allow the reader to pursue these aspects further.

It is of course impossible and futile to attempt to acknowledge the many individuals who have helped either directly or indirectly in the production of this book. The authors however wish especially to acknowledge members of the computer groups of the particle physics and nuclear structure divisions of the Nuclear Physics Laboratory at the University of Oxford for their invaluable help and cooperation. The authors are also grateful to the two other members of the Oxford microprobe group, G D Blower and J Takacs for their encouragements and comments on the text. We also wish to thank Professor K W Allen for providing the environment in which the work carried out for this book was stimulated.

G W Grime
F Watt
Oxford 1983

Contents

1

High-energy ion microprobes

1.1 Introduction

Several powerful analytical techniques are available when energetic ions impinge upon the surface of a specimen. If the energy of the incident ions is sufficiently high, then both atomic and nuclear processes can take place, which between them can provide simultaneous information on the elemental content of the sample over the whole periodic table, down to the parts per million level of sensitivity. Of the many reactions initiated by an incident ion beam of a few MeV in energy (figure 1.1), there are four mechanisms which are of primary interest:

(1) Proton- (or particle-) induced x-ray emission (PIXE)
(2) Elastic (or Rutherford) backscattering (RBS)
(3) Nuclear reactions
(4) Ion microscopy.

All four techniques will be discussed in sections 1.2 to 1.5, with the main emphasis on the processes

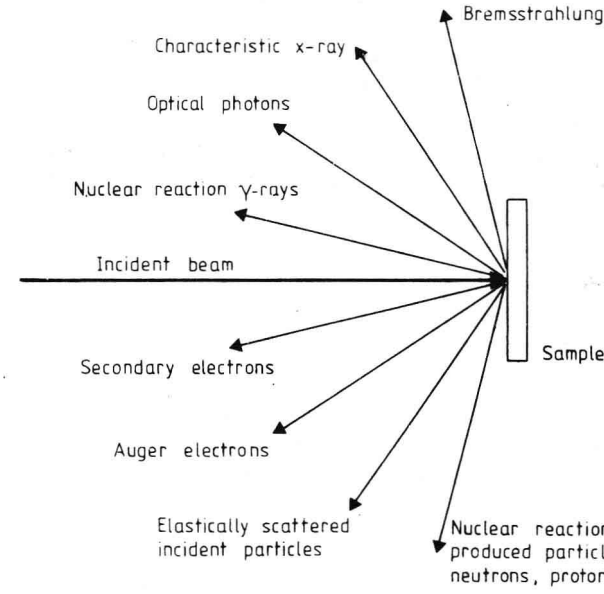

Figure 1.1 Schematic diagram of possible reactions initiated by an ion beam of MeV energy.

which have been shown to have major advantages over existing techniques, i.e. PIXE, RBS and nuclear reaction analysis techniques. Section 1.6 summarises the beam energy requirements for the analytical techniques considered. The advantages of focused ion microprobes should by then be apparent and subsequent sections will deal with the focusing of high-energy ion beams.

Section 1.7 deals with the concepts of brightness and emittance in beam optics and discusses the suitability of current ion sources for the production of ions in a form suitable for probes.

Section 1.8 considers the problem of ion-probe formation at the energies required by the techniques of PIXE, PBS and nuclear reaction analysis.

Section 1.9 describes very briefly and in simple terms, the action of the strong focusing quadrupole lens used in the probe formation.

Section 1.10 is a brief review of the beam optics terminology used extensively throughout the book.

Section 1.11 is a review of some microprobe systems in use at the time of writing. Since the subject matter of the book is concerned with beam optics, examples of the usage of microprobes are not considered. For information on specific applications and hardware, the reader should consult the respective references given in the section.

Lastly, section 1.12 is a brief review of the theoretical work carried out into quadrupole probe-forming systems. Again, the references listed in that section should be consulted for further information.

1.2 Proton-induced x-ray emission (PIXE)

X-ray emission used for analytical purposes has been known for some time, mainly in the form of x-ray fluorescence analysis, i.e. the induction of elemental characteristic x-rays by incident x-rays of higher energy. It was not until 1970 that Johansson *et al* [JO70a] showed that characteristic x-ray excitation by energetic protons, combined with detection of the x-rays by a solid-state detector cooled to liquid nitrogen temperatures constituted a powerful, multi-elemental analytical method of high sensitivity. For the reader who wishes a comprehensive review on PIXE there are several excellent review articles [JO76, FO78, FO75, ZI76, FO76a, FO76b] and published conference proceedings available [IO79, PI80, PI76].

Proton-induced x-ray emission is an atomic process (shown schematically in figure 1.2) in which there is a high probability of an inner-shell electron being ejected from an atom by an incoming proton.

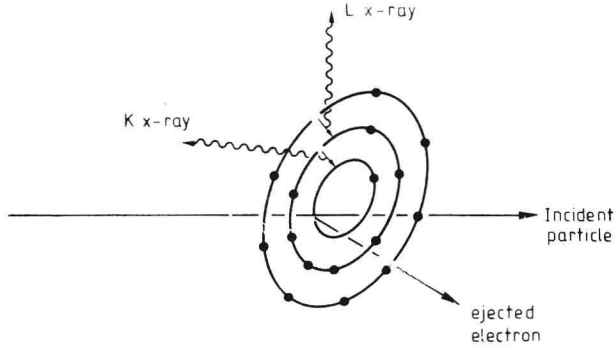

Figure 1.2 Schematic diagram showing the production of characteristic K and L x-rays by MeV ion collision.

The filling of the vacancy thus created by an electron from a higher shell causes an x-ray quantum to be emitted, the energy of which is characteristic of the atom under bombardment. The ability of a solid-state detector to resolve the

energies of adjacent characteristic x-rays with high efficiency and to detect simultaneously a wide range of x-rays gives us information on which elements are present in the analysed sample and in what quantities.

As a brief example to illustrate the power and versatility of this technique, we have chosen the analysis of a sample of environmental dust collected in the City of Oxford over a period of three days. Figure 1.3 shows an x-ray energy spectrum of the dust, induced by the bombardment of 4MeV protons from a nuclear accelerator. As a guide to the speed and sensitivity of PIXE for such environmental samples, elemental lead levels of about 0.1μg were obtained from this spectrum, which took only a few minutes to accumulate.

In laboratories where pollution studies are carried out routinely and require a fast sample turn-round time, the use of computer software [KA77, KA81, CL81] to extract absolute elemental quantities enables the composition of a sample to be obtained minutes after the end of a run.

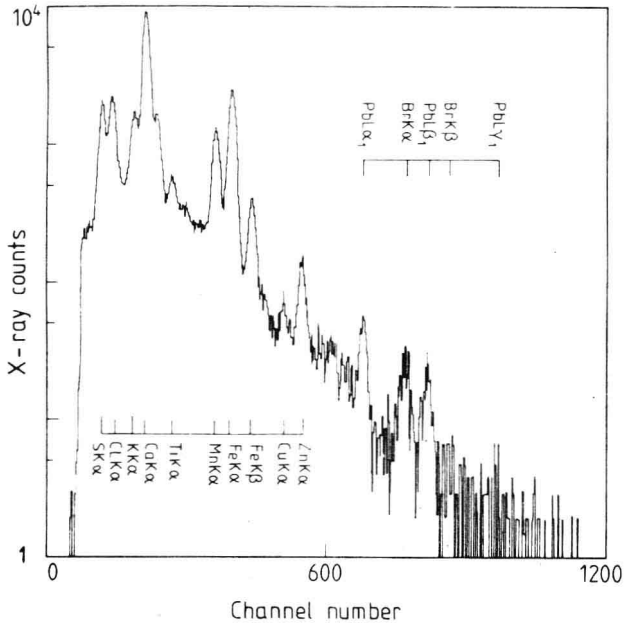

Figure 1.3 Proton induced x-ray energy spectrum from environmental dust. Proton energy = 4 MeV. Accumulated charge = 0.3 μC. Run times = 5 min.

The elemental constituents of a sample are identified through their characteristic x-ray energies and some of the prominent x-ray emission energies [JO70b] that are encountered in x-ray spectroscopy are listed in Appendix 2. From this table it is seen that the characteristic K_α x-ray energies corresponding to elements of low atomic number are small, and in practice the induced characteristic x-rays from the elements hydrogen to about sodium, (K_α x-ray energy = 1041 eV) are absorbed in the window of the detector assembly and any surface dead layer of the solid-state detector. Detection of low A elements is possible using a crystal spectrometer which has excellent energy resolution but which unfortunately has poor efficiency compared with that of solid-state detectors. Because it is a wavelength dispersive device, the analysis is not multi-elemental and a broad range of x-ray energies cannot be recorded simultaneously. From Appendix 2 it is also apparent that for elements above about Ga in the periodic table, elemental analysis can be achieved by observing the characteristic L x-rays (Ga L_α, x-ray energy = 1098keV). This is useful (as will be seen below) in order to maintain high elemental x-ray yields throughout the higher-mass region of the periodic table.

The dependence of inner-shell ionisation cross sections on incident particle energy has been extensively studied both theoretically and experimentally, with comparisons between the available theories and experiments in the energy and Z regions of interest good to within 10–30%. Johansson *et al* [JO76] have plotted data from K and L x-ray ionisation measurements on thin targets and fitted to the results a fifth degree polynomial of the form

$$\ln(\sigma u_i^2) = \sum_{n=0}^{5} b_n x^n \quad (i = \text{K or L})$$

where

$$x = \ln(E/\lambda u_i) .$$

u_i is the ionisation energy in eV

E is the proton energy in eV

σ is the ionisation cross section in units of 10^{-14} cm^2

λ is the ratio of the proton mass to the electron mass

u_L was calculated from

$$u_L = 1/4\ (u_{L_1} + u_{L_2} + 2u_{L_3})$$

and the b_n coefficients are given by

Shell	b_0	b_1	b_2
K	2.0471	−0.00659	−0.47448
L	3.6082	0.37123	−0.36971
Shell	b_3	b_4	b_5
K	0.09919	0.04606	0.00608
L	−0.00008	0.00251	0.00126

The relevant parameter for elemental analysis is the x-ray production cross section σ_p, related to σ by $\sigma_p = \sigma\omega k$ where ω is the fluorescent yield and k the relative intensity of possible transitions to fill an inner shell vacancy.

Figures 1.4 and 1.5 show plots of K_α and L x-ray production against proton energy for some common elements taken from values calculated by Johansson and Johansson [JO76] using the expressions above. Comparison of figures 1.4 and 1.5 show that due to the larger L x-ray cross sections for elements in the higher mass regions in the periodic table, observation of the characteristic L x-rays rather than the K x-rays for high-mass elements will result in more rapid analysis times.

It is seen from these graphs that, in general, the higher the proton energy the greater the x-ray production cross sections. The analytical sensitivity, however, is not only determined by the cross section but also by the x-ray background radiation, and the dominant part of this background radiation at low energies is the radiation caused by the deceleration of the secondary electrons ejected by incident particle impact (bremsstrahlung).

If E_e^m is the maximum energy transferred from an ion of mass M and energy E_p to a free electron of mass m then the bremsstrahlung background radiation decreases rapidly above the classical limit for free electron scattering given by

$$E_e^m = (4m/A_pM)\,E_p .$$

For example, E_e^m for a 2MeV proton is 4.36keV, corresponding approximately to the Sc K_α x-ray energy. By increasing the proton energy, therefore, although the x-ray production cross sections increase, so does the energy at which the bremsstrahlung background becomes significant.

The background caused by direct bremsstrahlung from the projectile is apparent only at higher radiation energies, being masked by the secondary electron bremsstrahlung up to the E_e^m cut-off energy. The cross section for this process is given by [JO76]:

$$\frac{d\sigma}{dE_x} = C\,\frac{AZ^2\,Z_1^2}{EE_x}\left(\frac{Z}{A} - \frac{Z_1}{A_1}\right)$$

where Z, A, and E are the charge, mass and energy respectively of the incident particle, E_x is the x-ray

energy and Z_1 and A_1 the charge and mass of the target atoms. Note that the yield, unlike that of the secondary electron bremsstrahlung, increases with decreasing particle energy.

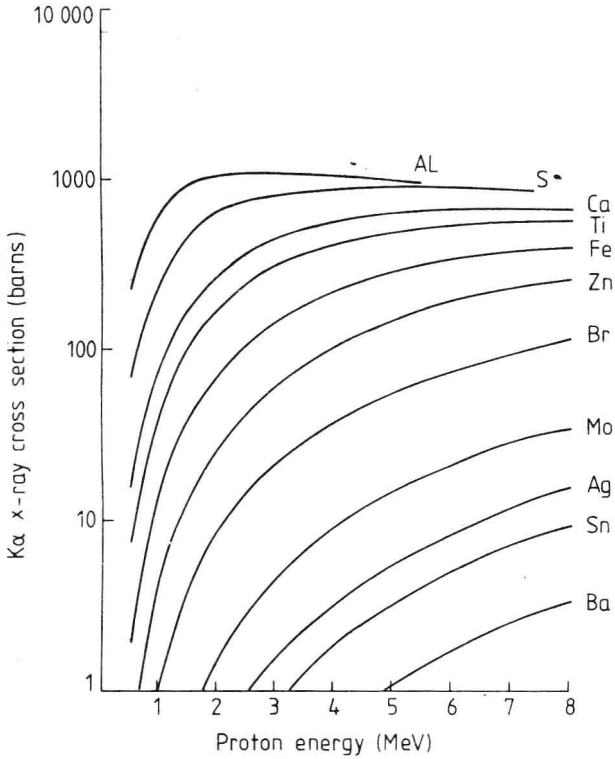

Figure 1.4 Plot of K_α x-ray production cross sections against incident proton energy for several common elements.

A third important source of background, which again is only noticeable at higher x-ray energies, is when the incident particles have a sufficiently high energy to produce nuclear reaction γ-radiation in the target. This nuclear background produces a high-energy tail in the spectrum due to Compton scattering in the detector.

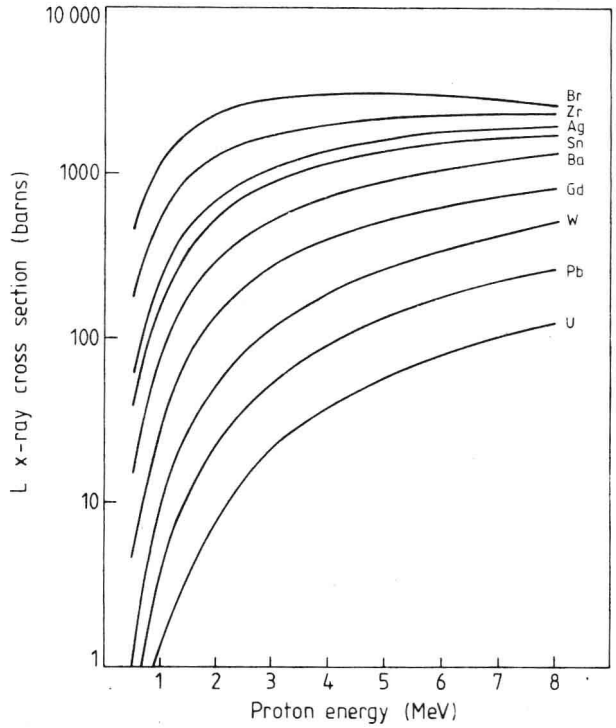

Figure 1.5 Plot of L x-ray production cross-sections against incident proton energy for several common elements.

The optimum incident particle energy for maximum sensitivity in PIXE is therefore balanced between higher incident energies for increased x-ray production cross sections and reduced incident energies to minimise background. In general, most PIXE work is carried out with proton energies between 2 and 6 MeV. The figures for optimum concentration sensitivities and absolute detection limits of an element in a sample are dependent on several factors. Sensitivity, and therefore absolute detection limits are degraded by:

(1) The target thickness: in general, the thicker the target the greater the secondary electron bremsstrahlung radiation.

(2) Low x-ray production cross sections: although for elements in the high Z range, the more prolific L x-rays can be utilised.
(3) Target constituents: multi-elemental targets can be difficult to analyse because of overlapping K_α, K_β and L x-ray lines.
(4) Electronic pile-up: spurious counts due to overlapping or coincident pulses at high count rates. This is a common occurrence for trace element analysis in medium to high Z matrices where the prolific x-rays from the matrix material cannot be filtered out. This problem, however, is not so great for elemental analysis of biological material, where the energies of the x-rays from the main bulk of the sample are below the threshold of detection.
(5) Detector resolution: currently available resolutions of 140 eV at 5.9 keV x-ray energy are adequate for separating K x-ray peaks down to the detection threshold. Poorer resolution due to electronic noise, large area silicon crystals, inferior pulse processing etc may result in overlapping peaks.
(6) Sample charging: internal or surface charging of a sample caused by beam bombardment may cause localised intense electric fields which can increase energy of any secondary electrons above the E_c^m cut-off thereby extending the range of the secondary electron bremsstrahlung background.
(7) Primary particle bremsstrahlung.
(8) Nuclear reaction Compton scattering.
(9) Associated with any intense x-ray peak from a major elemental constituent is a low-energy tail caused by incomplete charge collection within the detector and Compton scattering of the primary x-ray.

Folkmann [FO78] has made an attempt to calculate concentration sensitivities and absolute detection limits using, as a model, trace elements embedded in several different elemental matrices of thickness 1 mg cm^{-2}. Using x-ray production cross section data, together with calculated secondary electron and incident particle bremsstrahlung backgrounds, he concluded that the optimum concentration sensitivity is in the region 10^{-6}–10^{-7} within a Z range that can be moved with beam energy. The absolute detection limit is easily deduced by multiplying the concentration sensitivity by the matrix thickness (mass/area) and the beam area. For a typical concentration sensitivity of 10^{-6}, target thickness of 1–0.1 mg cm^{-2} and incident beam areas of 1 cm^2–1 mm^2, then trace elements in the range 10^{-9}–10^{-12} g are detectable. It is perhaps interesting to note at this stage that for a beam focused down to 1 μm while maintaining the 10^{-6} sensitivity and assuming no target damage, the detection limit is 10^{-18} g!

In summarising the analytical power of proton-induced x-ray emission we have:

(1) Fast.
(2) High concentration sensitivity for elements above $Z = 11$ (10^{-6}–10^{-7}).
(3) Low minimum detectable concentrations (routinely 10^{-9}–10^{-12} g).
(4) Multi-elemental: information on elemental composition of the sample is obtained simultaneously.
(5) Elements can be identified easily by their characteristic x-ray energies.
(6) Microbeams can be used. This not only decreases the minimum detectable concentration but as we shall see later, enables two-dimensional elemental mapping to be carried out.
(7) Essentially non-destructive (apart from possible damage in some applications, e.g. intense microprobe beam-mapping of biological material).

The comparison between proton-induced x-ray emission and other analytical techniques has been carried out recently by several groups. Deconninck *et al* [DE81] have investigated the trace element content of albumin using PIXE and compared the results with those obtained by atomic absorption spectroscopy (AAS), a standard medical laboratory technique, for which commercial instruments are available. The conclusions drawn from the comparisons were the same as we have experienced in Oxford in monitoring rubidium levels in blood cells and plasma using PIXE and AAS: AAS is subject to practical difficulties in which inaccuracies occur due to varying flame intensity, background instabilities etc. Nevertheless, under the control of an experienced operator, the technique is as good as, if not superior to, PIXE as an analytical technique in the detection of a single element only.

Several groups [BU81, CO73, GO73, GI73] have measured trace element concentrations in samples using both PIXE and x-ray fluorescence (XRF). The techniques are basically similar in that PIXE uses energetic ions to induce the characteristic elemental x-rays whereas XRF uses x-rays either from an x-ray tube or a radioactive source. A comparison between the sensitivities of these two multi-elemental techniques across the periodic table is difficult because of the differences in the x-ray background of the two processes. As discussed above, in PIXE the major source of background is of low-energy character, corresponding to the bremsstrahlung generated by secondary electrons. In XRF the problem is with the Compton scattering of the primary x-ray radiation which is essentially high energy in character [WO73]. In general, the concentration sensitivities in both processes seem to be similar, providing the energy of the excitation source is optimised. When considering minimum detection limits on an absolute scale, however, the superiority of PIXE is pronounced. When using tube-produced x-rays, and x-rays from a radioactive source, the incident photon flux is much smaller than that of accelerator-produced protons over a given area. XRF then requires thicker samples, which also introduce matrix effects (absorption of the emitted x-rays in the bulk of the material) into the technique, thereby complicating the analysis. In cases where the sample mass is small (e.g. pollution targets, biological tissue, semiconductor material etc) the lower detectable limits of PIXE are necessary, although there are many materials analysis problems for which the relatively less complex XRF is more than adequate.

Neutron activation analysis (NAA) is a powerful technique with sensitivities superior to PIXE for certain elements. The sample is bombarded with neutrons and the trace element identification is carried out by observing characteristic γ-decay of short-lived product radionuclides. Maenhaut *et al* [MA81a] have investigated the trace element content of serum, serum albumin and living tissues with both PIXE and NAA. They conclude that the two techniques are complementary, in that more trace elements could be determined using both PIXE and NAA than by using one technique alone.

The three techniques described above, AAS, XRF and NAA, have been compared to PIXE because they achieve more or less equivalent concentration sensitivities although they are inferior in the minimum detectable concentration limits. There are obviously many more analytical techniques available, most of which involve low-energy electrons, ions or photons as the incident or analysed radiation and are hence surface techniques, and it is outside the scope of this book to consider them all.

As we have seen, the ability to focus protons down to small spot sizes improves the minimum detectable concentration drastically and it is because of this that PIXE offers more potential for small sample analysis than AAS, XRF and NAA. This, however, is not the only advantage. The ability to focus a proton beam to a small spot and scan a

sample while observing characteristic x-rays enables two-dimensional elemental mapping to be carried out.

The technique of electron-induced characteristic x-ray emission has this capability and for many years electron microscopists have utilised the detection of x-rays in conjunction with secondary electrons to enable mapping of elemental concentrations in samples. Unfortunately, the large unavoidable x-ray background caused by the bremsstrahlung of the primary electrons degrades the concentration sensitivity to only one part in 10^3–10^4, thereby allowing only the major elemental constituents to be detected. A comparison of x-ray spectra of a pollen tube taken using both 2.5MeV protons and 10keV electrons is given in work carried out by the Heidelberg group [BO80a] showing the differences in sensitivity of the two techniques to trace element analysis.

The proton probe therefore seems to offer a unique service, that of two-dimensional trace element mapping for elements with $Z>11$ at concentration levels of parts per million.

1.3 Particle-induced nuclear reactions

The use of nuclear reactions for elemental analysis is an expanding field and covers a broad range of reaction mechanisms. A nuclear reaction is usually written in the form A(B,C)D where A+B→C+D + Q, with A the target nucleus, B the incident particle, C the reaction product and D the residual nucleus. Q is the energy released during the reaction as particle kinetic energy or γ-radiation, or absorbed from the incident particle energies. The elements under investigation are identifiable through the energy of the reaction products in the same way that an excited atom is identified through its characteristic x-ray radiation. Because the Q-values of nuclear reactions vary so dramatically even for elements adjacent in the periodic table [MA66] and the lowest excited states of the light nuclei are in general widely spaced and well defined [LE76a], the reaction products have distinctive energies and are therefore easily recognisable. An added advantage is that nuclear characteristics differ markedly between isotopes of the same element and so the reaction products are specific to a particular isotope of that element. Figure 1.6 shows a schematic diagram of the possible nuclear reactions that can take place and for an excellent review of the subject the reader is referred to an article by Wolicki [WO75].

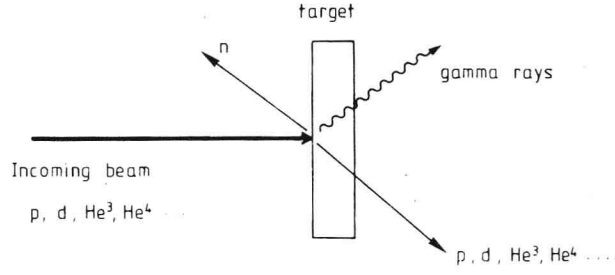

Figure 1.6 Schematic diagram of the production of nuclear reaction particles induced by an ion beam of MeV energy.

For particle-induced nuclear reaction cross sections to be high enough for useful elemental analysis, the incident particle must have sufficient energy to overcome the electrostatic potential energy which builds up as it approaches a target nucleus. The height of this Coulomb barrier for a

particle of charge Z_1e and radius R_1 impinging on a target nucleus of charge Z_2e and radius R_2 is given by

$$E_C = \frac{Z_1 Z_2 e^2}{(R_1 + R_2)4\pi\varepsilon_0}$$

where

$R_1 + R_2 = R$, the interaction radius

$= R_0 (A_1^{1/3} + A_2^{1/3})$

where A_1, A_2 are the mass numbers of the nucleus and the incident particle. In general, R_0 lies between 1.0 and 1.4 fm. (An approximate but useful estimate of the Coulomb barrier height per incident nuclear charge is $E_C = ZA^{-1/3}$MeV.) For a given incident beam particle, the barrier height is greater as the atomic number of the target nucleus increases. In general, if the most readily available lightest particles (p,d, ^{3}He and ^{4}He) are used, then, at incident particle energies of about 4MeV, the Coulomb barrier will only be overcome for target atoms of atomic number up to about 20, and therefore at these comparatively economic energies it is only for these light elements that the nuclear reaction cross sections can be high.

It is interesting to point out at this stage the remarkable complementary relationship between analysis using nuclear reactions and PIXE. As we have already seen, in PIXE, elements below $Z = 11$ are in general not detected because their characteristic x-ray energies are so low that they are absorbed before detection. The PIXE technique, therefore, is most efficient in detecting heavy trace elements of $Z > 11$ embedded in a light matrix of $Z < 11$. In nuclear reaction analysis, however, the cross sections are small for elements of $Z > 20$, due to the effects of the nuclear Coulomb potential, and so this analytical technique is most sensitive for light elements embedded in a heavy matrix.

Analysis using nuclear reactions can be divided into two distinct types; charged particle activation analysis (CPAA) and prompt radiation analysis (PRA).

In charged particle activation analysis, the residual nucleus is left in a state of radioactivity and the decay products of the excited nucleus are measured some time after the reaction. The identifying characteristics for the radioactive nucleus can be the half-life for decay, the types of radiation emitted and the characteristic γ-rays emitted from the daughter nucleus. The concentration sensitivities for this technique can be better than one part per million for many light elements [TI66, MA62, DE71, AA72]. For obvious reasons, it is not a technique where elemental mapping can be carried out, and therefore the interest in using the method in conjunction with a focused beam is limited. The reader is therefore referred to a comprehensive bibliography [LU71] on activation analysis if he wishes to pursue the subject further.

Prompt radiation analysis (PRA) is a technique in which an element in a sample is detected through the nuclear radiations emitted instantaneously from nuclear reactions induced by the incident particle beam. In many respects, the experiments resemble those of early nuclear structure research although the objectives are clearly different.

Nuclear reactions can be broadly categorised into three basic mechanisms. The first of these is termed a capture reaction in which the incident particle is captured by the target nucleus to form a compound nucleus which subsequently decays by the emission of one or more γ-rays, e.g. ^{20}Ne $(\alpha, \gamma)^{24}$Mg. The second is the inelastic scattering of the incoming particle in which some of the kinetic energy of the particle is absorbed by the target nucleus, which subsequently decays by γ-emission, e.g. ^{12}C(p,pγ)^{12}C. The third category is when the particles which separate after the reaction are not the same as the incident particle and target nucleus, e.g. ^{19}F(p,α)^{16}O.

The great variety of ways in which information about a target sample can be obtained through nuclear reactions is indicated by the vast quantity of